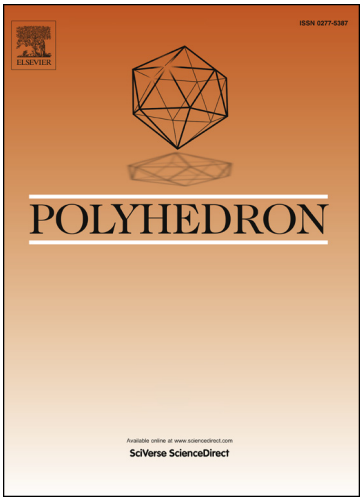

Zn(II) coordination compounds derived from 4-acyl pyrazolones and 1, 10 phenanthroline: Syntheses, crystal structures, spectral analysis and DNA binding studies

R.N. Jadeja, Mitesh Chhatrola, Vivek K. Gupta

PII: S0277-5387(13)00543-3
DOI: http://dx.doi.org/10.1016/j.poly.2013.07.018
Reference: POLY 10249

To appear in: *Polyhedron*

Received Date: 20 April 2013
Accepted Date: 11 July 2013

Please cite this article as: R.N. Jadeja, M. Chhatrola, V.K. Gupta, Zn(II) coordination compounds derived from 4-acyl pyrazolones and 1, 10 phenanthroline: Syntheses, crystal structures, spectral analysis and DNA binding studies, *Polyhedron* (2013), doi: http://dx.doi.org/10.1016/j.poly.2013.07.018

Zn(II) coordination compounds derived from 4-acyl pyrazolones and 1, 10 phenanthroline: Syntheses, crystal structures, spectral analysis and DNA binding studies

R. N. Jadeja[a*], *Mitesh Chhatrola*[a], *Vivek K. Gupta*[b]

[a]*Department of Chemistry, Faculty of Science, The M. S. University of Baroda, Vadodara 390 002, India*

[b]*Post-Graduate Department of Physics & Electronics, University of Jammu, Jammu Tawi 180 006, India*

*E-mail- rajendra_jadeja@yahoo.com, Tel: +91-265-2795552 ext 30

Abstract

A new series of three Zn(II) coordination complexes [Zn(MCPMPAC)$_2$H$_2$O] = complex **1**, [Zn(PMPAC)$_2$H$_2$O] = complex **2** and [Zn(PMPAC)$_2$(phen)] = complex **3** (MCPMPAC = 4-acyl-3-methyl-1-(3-chlorophenyl) pyrazolone-5-one, PMPAC = 4-acyl-3-methyl-1-phenyl pyrazolone-5-one, Phen = 1, 10 phenanthroline) has been synthesized and characterized. The structural features of synthesized complexes were determined by metal estimation, molar conductivity, IR, UV–Visible, NMR and single crystal X-ray study. The conductivity data confirm the non-electrolytic nature of the complexes. The single crystal analyses of the complexes show that the Zn(II) ion is five-coordinated with water molecule at axial position in case of **1** and **2** whereas, six-coordinated with phenanthroline ligand in case of **3**. Binding of the synthesized complexes with calf thymus DNA (CT-DNA) was studied by spectroscopic methods and viscosity measurements. Experimental results suggest that the zinc complexes have the ability to form adducts with DNA and to distort the double helix by changing the base stacking.

Keywords: 4-propionyl pyrazolone, Zn(II) complex, Crystal structure, DNA binding study

1. Introduction

Structural investigation of the binding modes of the ligands in ternary transition metal complexes is of great interest due to their effect on the topologies and propagation of extended coordination compounds [1]. This area of research has evolved rapidly in recent years as the coordination compounds may have interesting properties and applications, e.g., DNA Binding, Cleavage and other biological applications [2]. On the other hand, studying the interactions of metal ions with drugs and biologically active ligands is important to investigate the potential for synergistic activity between the metal and the drugs as well as understanding the toxic side effects of synthetic drugs which may, in part, be arising due to these interactions [3]. Pyrazolone nucleus, which is very useful pharmacological ingredient, especially to the class of non-steroidal anti-inflammatory drugs (NSAIDs) is used in the treatment of arthritis and other musculoskeletal joint disorders and ear preparations [4]. Coordination chemistry of 4-acyl pyrazolones has been previously investigated where it has been used as a blocker for coordination compounds and for synthesis of biologically active complexes [5]. Their metal complexes have been found to display catalytic performance, biological activity and photochromic properties. The focus of our research on transition metal complexes with pyrazolone derivatives is due to the theoretical and practical significance of these compounds. A number of pyrazolone derivatives show biological activity, as a consequence, some are commercial products or compounds in the phase of activity evaluation. As part of our investigations on metal pyrazolone systems, we have previously examined the ligation behavior of various 4-acyl 3-methyl-1-phenyl-pyrazolone-5-one and their derivatives with different metal ions like Ca, V, Cr, Mn, Fe, Ni, Cu [6-12].

In this work, we have extended our study to the synthesis of binary and mixed-ligand complexes of Zn(II) metal with 4-propionyl-pyrazol-5-one ligands and chelating heteroaromatic N-donor ligand 1, 10 phenanthroline. We here in report the synthesis,

characterization and crystal structures of three zinc acyl pyrazolone complexes, in which the components are 4-propionyl-pyrazolone ligands and 1, 10 phenanthroline (phen).

2. Experimental

2.1. Materials

The reagents and chemicals of analytical reagent grade were procured from commercial sources. Solvents used for electrochemical and spectroscopic studies were purified using standard procedures [13]. 1, 4 dioxane was obtained from E. Merck (India) Ltd. Calcium hydroxide, zinc acetate and 1, 10 phenanthroline were obtained from LOBA Chem. Pvt. Ltd., Mumbai and used as supplied. Absolute alcohol was obtained from Baroda Chem. Industry Ltd. and was used after distillation. Methanol was obtained from Spectrochem. Mumbai, India and was used after distillation. CT-DNA (Calf Thymus DNA) was purchased from Sigma Aldrich. Ethidium bromide (EB) was obtained from Hi-media laboratories Pvt. Ltd., Mumbai.

2.2. Methods

The synthesized compounds were characterized using different techniques. Infrared spectra (4000-400 cm^{-1}, KBr discs) of the samples were recorded on a model RX 1 FTIR Perkin-Elmer spectrophotometer. ^{1}H NMR spectra of the ligands were recorded with Bruker AV 400 MHz using $CDCl_3$ as a solvent and TMS as an internal reference. ^{1}H NMR spectra of complex **3** was recorded with Bruker AV 400 MHz using $CDCl_3$ as a solvent, ^{1}H NMR spectra of complexes **1** and **2** were recorded with Bruker AV 400 MHz using DMSO as a solvent and Mass spectra of the ligands were recorded on Trace GC ultra DSQ II. The electronic spectra (in DMF at room temperature) in the range of 400-800 nm were recorded on a model Perkin Elmer Lambda 35 UV-VIS spectrophotometer. Fluorescence spectra were recorded on a model JASCO, FP-6300 fluorescence spectrophotometer. Molar conductivity of 10^{-3}M solution of the complexes in DMF was measured at room

temperature with a model Elico CM 180 digital direct reading deluxe digital conductivity meter. Zinc content was determined by gravimetric analysis after decomposing the complexes with HNO_3.

2.3. Synthesis of ligands

2.3.1. 4-propionyl-3-methyl-1-phenyl pyrazolone-5-one (PMPAC)

3-methyl-1-phenyl pyrazolone-5-one (0.1 mol, 17.4gm) was dissolved in hot dioxane (80 cm^3) in a flask equipped with a stirrer, separating funnel and reflux condenser. Calcium hydroxide (0.2 mol, 14.81gm) was added to this solution, followed by acetyl chloride (0.1 mol, 8.684 cm^3) added drop wise with precaution, as this reaction was exothermic. During this addition the whole mass was converted into a thick paste. After the complete addition, the reaction mixture was refluxed for half an hour and then it was poured into dilute hydrochloric acid (2 M, 200 cm^3). The colored crystals (PMPAC) thus obtained were separated by filtration and recrystallized from an acidified methanol–water mixture (HCl:MeOH:H_2O = 1:80:19). M.P. 90°C, Yield 80.85 %, Molecular formula:$C_{13}H_{14}N_2O_2$ (calc.M.W. 230.26); Mass: m/z = 230.02 [$C_{13}H_{14}N_2O_2$, MIP]$^+$, 231.26 [$C_{13}H_{14}N_2O_2$ (m+1) Peak]$^+$, 200.62 [$C_{11}H_8N_2O_2$ Base peak]$^+$, 201.31 [$C_{11}H_9N_2O_2$]$^+$, 82.70 [$C_3H_3N_2O$]$^+$, 137.20 [$C_7H_{10}N_2O$]$^+$, 68.90 [C_5H_5]$^+$, 56.99 [C_4H_8]$^+$; IR (KBr, cm^{-1}): 1563(s) (C=N, cyclic), 1635 (m) (C=O, Pyrazolone ring), 1651 (m) (C=O, Propionyl group); ^{1}H NMR ($CDCl_3$): 1.24-1.28 (t) (3H, Propionyl C-CH_3), 2.48 (s) (3H, Pyrazolone C-CH_3), 2.77-2.82 (q) (2H Propionyl-CH_2-), 7.27-7.85 (m) (5H Phenyl), 11.695 (s) (1H, Phenolic –OH).

2.3.2. 4-propionyl-3-methyl-1-(3-chlorophenyl) pyrazolone-5-one (MCPMPAC)

It was analogously prepared from 3-methyl-1-(3-chlorophenyl) pyrazolone-5-one. The colored crystals thus obtained were separated by filtration and recrystallized from an acidified methanol–water mixture (HCl: MeOH: H_2O = 1:80:19). M.P. 86°C, Yield 69.6 %, Molecular formula $C_{13}H_{13}ClN_2O_2$ (calc.M.W. 264.70); Mass: m/z = 264.08 [$C_{13}H_{13}ClN_2O_2$, MIP]$^+$,

266.08 [$C_{13}H_{13}ClN_2O_2$ (m+2) Peak]$^+$, 263 [$C_{13}H_{13}ClN_2O_2$ (m-1) Peak]$^+$, 236.15 [$C_{11}H_9ClN_2O_2$]$^+$, 85.07 [$C_3H_4N_2O$]$^+$, 96.81 [$C_4H_4N_2O$]$^+$, 68.93 [C_5H_8]$^+$, 219.21 [$C_{12}H_{14}N_2O_2$]$^+$, 56.92 [C_4H_8, Base peak]$^+$, 125.15 [$C_6H_8N_2O$]$^+$, 42.96 [C_3H_6]$^+$; IR (KBr, cm^{-1}): 1563(s) (C=N, cyclic), 1634 (m) (C=O, Pyrazolone ring), 1651 (m) (C=O, Propionyl group); ^{1}H NMR ($CDCl_3$): 1.25-1.29 (t) (3H, Propionyl C-CH_3), 2.48 (s) (3H, Pyrazolone C-CH_3), 2.77-2.82 (q) (2H, Propionyl –CH_2-), 7.24-7.93 (m) (4H, Phenyl group), 11.65 (s) (1H, Phenolic –OH).

Synthesis of ligands is summarized in scheme 1.

2.4. Syntheses of Zn(II) complexes

2.4.1. Synthesis of 1

The complex was synthesized by the following method. The metal salt Zinc-acetate [$Zn(CH_3COO)_2.2H_2O$] (0.219 gm, 0.001 mmol) was dissolved in methanol and the solution was added to a cool methanolic solution of the ligand (MCPMPAC) (0.528gm, 0.002 mmol). After complete addition, the mixture was refluxed about for 4 hours. The reaction mixture was then filtered and was washed with Et_2O and water and dried in air. It was recrystallized from DMF at RT. M.P. 210'C, Yield 79.2 %, Molecular formula: $C_{26}H_{26}Cl_2N_4O_5Zn$ (calc.M.W. 632.87); IR (KBr, cm^{-1}): 3109 (co-ordinated H_2O), 1615 (C=O Propionyl group), 1555 (C=N cyclic), 1485 (C-O, pyrazolone ring), 511 (Zn-O); ^{1}H NMR ($CDCl_3$): 1.063-1.026 (t) (6 H, C-CH_3 Propionyl group), 2.703-2.648 (q) (4H,-CH_2-CH_3 Propionyl group), 2.300 (s) (6H, -CH_3 methyl group), Benzene ring 7.140-7.121 (d) (2H), 7.362-7.322 (t) (2H) 7.882-7.861 (d) (2H), 8.161 (s) (2H).

2.4.2. Synthesis of 2

It was analogously prepared from $Zn(CH_3COO)_2.2H_2O$ (0.219 gm, 0.001 mmol) and PMPAC (0.460gm, 0.002 mmol). It was recrystallized from DMF at RT. M.P.170-175'C, Yield. 69.33 %, Molecular formula: $C_{26}H_{32}N_4O_5Zn$ (calc.M.W. 545.965); IR (KBr, cm^{-1}):

3060 (co-ordinated H_2O), 1615 (C=O Propionyl group), 1505 (C=N cyclic), 1416 (C-O bond pyrazolone ring), 510 (Zn-O); ^{1}H NMR ($CDCl_3$): 1.035-1.072 (t) (3 H, C-CH_3 Propionyl group), 2.634-2.689 (q) (2H,-CH_2-CH_3 Propionyl group), 2.317 (s) (3H, -CH_3 methyl group), Benzene ring 7.971-7.951 (d) (2H), 7.346-7.307 (t) (2H) 7.123-7.086 (t) (1H).

2.4.3. Synthesis of 3

The complex was synthesized by the following method. The metal salt Zinc- acetate ($Zn(CH_3COO)_2.2H_2O$) (0.219 gm, 0.001 mmol) was dissolved in methanol and the solution was added to a hot methanolic solution of the ligand (PMPAC) (0.460gm, 0.002 mmol) and 1, 10 phenanthroline (0.198 gm, 0.001 mmol). After complete addition, little amount of sodium acetate was added and the mixture was refluxed about for 5 hours and after some time crystalline solid was obtained. The mixture was then filtered and washed with hot water and dried in air. It was recrystallized from DMF. M.P. 230ºC, Yield 61.42%, Molecular formula: $C_{38}H_{38}N_6O_4Zn$ (cacl.M.W. 708.15); IR (KBr, cm^{-1}): 1635 (m) (C=O Propionyl group), 1555 (s) (C=N cyc lic), 1485 (C-O, pyrazolone ring), 511 (Zn-O), 422 (Zn-N); ^{1}H NMR ($CDCl_3$): 1.003-0.965 (t) (3H, C-CH_3 Propionyl group), 2.611-2.556 (q) (2H,-CH_2-CH_3 Propionyl group), 2.367 (s) (3H, -CH_3 methyl group), Benzene ring 7.226-7.188 (t) (2H), 7.047-7.029 (t) (1H), 9.247-9.239 (d) (1H), 8.479-8.454 (d) (1H), Phenanthroline ring 7.953-7.846 (m) (4H).

Synthesis of complexes is summarized in scheme 2.

2.5. Crystallography

Crystals having good morphology were chosen for three-dimensional intensity data collection. X-ray intensity data of the complexes were collected at room temperature on Bruker CCD area-detector diffractometer equipped with graphite monochromated MoKα radiation (α=0.71073 Å). The crystals used for data collection was of suitable dimensions 0.30x0.20 x0.20 mm. The unit cell parameters were determined by least-squares refinement.

Data were corrected for Lorentz, polarization and multi-scan absorption correction [14]. The structures were solved by direct methods using SHELXS97 [15]. All non-hydrogen atoms of the molecules were located in the best E-map. Full-matrix least-squares refinement was carried out using SHELXL97 [15]. Hydrogen atoms were placed at geometrically fixed positions and allowed to ride on the corresponding non-H atoms with C-H = 0.93-0.96Å, and Uiso=1.5 Ueq of the attached C atom for methyl H atoms and 1.2 Ueq for other H atoms. An ORTEP [16] view of the complexes with atomic labeling is shown in Fig. 1. The geometry of the molecules has been calculated using the software PLATON [17] and PARST [18]. The crystallographic data for the complexes are summarized in Table 1. The important bond lengths and bond angles of the complexes are listed in Table 2.

2.6. DNA binding

All of the experiments involving the binding of complexes with CT-DNA were carried out in double distilled water with trisodium citrate (Tris, 15 mM) and sodium chloride (150 mM) and adjusted to pH 7.05 with hydrochloric acid. The DMF solution of the complex was used throughout the study. The concentration of CT-DNA per nucleotide was estimated from its known extinction coefficient at 260 nm (6600 M^{-1} cm^{-1}) [19]. Solutions of CT-DNA in tris buffer gave a ratio of UV absorbance at 260 and 280 nm (A_{260}/A_{280}) 1.8-1.9 indicating that the DNA was sufficiently free of protein. Absorption titration experiments were performed by maintaining a constant metal complex concentration (5 μM), while gradually increasing the concentration of DNA (0−75 μM). While measuring the absorption spectra, an equal amount of DNA was added to both the test solution and the reference solution to eliminate the absorbance of DNA itself.

The data were then fit to eq 1 [20] to obtain intrinsic binding constant K_b.

$$[DNA]/(\varepsilon_a - \varepsilon_f) = [DNA]/(\varepsilon_b - \varepsilon_f) + 1/K_b\ (\varepsilon_b - \varepsilon_f) \quad \ldots\ldots (1)$$

Where, [DNA] is the concentration of DNA in base pairs, $_a$ is the extinction coefficient observed for the MLCT absorption band at the given DNA concentration, $_f$ is the extinction coefficient of the complex free in solution, and $_b$ is the extinction coefficient of the complex when fully bound to DNA. A plot of [DNA]/[$_a$- $_f$] versus [DNA] gave a slope 1/[$_a$- $_f$] and Y intercept equal to (1/K_b)[$_b$- $_f$], respectively. The intrinsic binding constant K_b is the ration of slope to intercept [20].

Competitive studies of compound with ethidium bromide (EB) have been investigated with fluorescence spectroscopy in order to examine whether the compound can displace EB from its CT DNA−EB complex. The CT DNA−EB complex was prepared by adding 3.3 μM EB and 4.2 μM CT-DNA in buffer (150 mM NaCl and 15 mM trisodium citrate at pH 7.05). The intercalating effect of the compound with the DNA−EB complex was studied by adding a certain amount of a solution of the complex step by step (0-370 μM) into the solution of the DNA−EB complex. The influence of the addition of each complex to the DNA−EB complex solution has been obtained by recording the variation of fluorescence emission spectra. The emission spectra were monitored by keeping the excitation of the test compound at 546 nm and the emission was monitored in the range of 550-750 nm. The emission was observed at 610 nm.

Commonly, fluorescence quenching can be described by the following Stern−Volmer equation (eq 2) [21].

$$F_0/F = 1 + K_{sv}[Q] \quad \ldots\ldots (2)$$

Where F_0 and F are the steady-state fluorescence intensities in the absence and presence of quencher, respectively, K_{sv} is the Stern-Volmer quenching constant, obtained from the slope of the plot F_0/F versus [Complex] and [Q] is the total concentration of quencher.

Viscosity experiments were carried out by using an auto viscometer (SCHOOT AVS 350), immersed in a thermostated water bath with the temperature setting at 30 ± 1 ˚C for 15 min. DNA samples with an approximate average length of 200 base pairs were prepared by sonication in order to minimize complexities arising from DNA flexibility [22]. The concentration changes of the Zn(II) complexes were realized by adding different volumes of Zn(II) complex stock solution. Flow time was measured with a digital stopwatch, and each sample was measured triply, and an average flow time was obtained. Data were presented as $(\eta/\eta_o)^{1/3}$ versus the mole ratio of Zn(II) complex to DNA. Where η is the viscosity of DNA in the presence of complex, and η_o is the viscosity of DNA alone.

3. Results and discussion

The pyrazolone derivatives were prepared by refluxing an appropriate amount of respective 3-methyl-pyrazolone-5-one with the Propionyl chloride. The structures of the synthesized ligands were established with the help of IR, NMR, and Mass spectra. All spectral data are agreed well with the acyl pyrazolone ligand structures. All Zn(II) complexes were prepared by using the metal salt with the corresponding ligands in molar ratio of metal:ligand as 1:2 as obtainable in the following reaction.

$$M\cdot(CH_3COO)_2\cdot nH_2O + 2L \rightarrow ML_2 + nH_2O + nCH_3COOH$$

where, M= Zn(II)

All these complexes are colorless, air and moisture free amorphous solids. They are insoluble in common organic solvents and only soluble in DMF and DMSO. Molar conductance values of the soluble complexes in DMF (10^{-3}M solution at 25 ◦C) indicate that the complexes have molar ratio of metal:ligand as 1:2. The lesser molar conductance values 7.00 for **1**, 5.00 for **2** and 15.00 for **3** ohm^{-1} cm^2 mol^{-1} indicate that they are all nonelectrolytic in nature [23]. The elemental analyses data concur well with the planned formulae and also recognized the $[ML_2 (H_2O)]$ composition for **1** and **2** complexes and $[ML_2$

(Phen)] composition for **3** complex. All the complexes were characterized by FT-IR, NMR, Single crystal analyses and UV–Visible spectroscopic techniques. Analytical data of the synthesized complexes and ligands are given in section 2.

3.1. Spectroscopy

The IR spectral studies provide valuable information regarding the coordinating sites of ligand. The IR spectra of the complexes were compared with that of the free ligand to determine the changes that might have taken place during the complexation. A comparative study of the IR spectra of ligands and its metal complexes reveals that certain bands are common and therefore, only important bands, which have been either shifted or newly appeared, are discussed. In the free ligand, a medium-intensity band at 3011cm^{-1} which assigned to enol *v*(OH) of β-diketone tautomer is absent in complex. A band at 1626 cm^{-1} in the free ligand is allocated as *v*(C=O) of pyrazolone-ring transfers to 1485 cm^{-1} in the complex [24]. The band at 1651cm^{-1} in Propionyl group changes to 1615 cm^{-1} in the complex. IR spectral evidence, therefore, suggests that the enolic proton of ligand is replaced by Zn(II) in the complex. FT-IR spectra of ligands exhibits the bands within the range 1550–1565 cm^{-1} which can be assign to *v*(C=N) (cyclic). The complexes show the absorption within 3000–3150 cm^{-1} which can be assigned to the coordinated water molecules. The complexes show bands at 510 cm^{-1} and 422 cm^{-1} which are due to the *v*(Zn-O) and *v*(Zn-N), respectively [25]. The IR spectral data are shown in section 2.

The ^{1}H spectra of both the ligands were recorded in $CDCl_3$ at room temperature. The signals due to one methyl group appeared as singlet in the range 2.38–2.47 *ppm*. In the aromatic region, a few doublets and in few cases some overlapping doublets/multiplets are observed in the range 7.25–7.99 *ppm* in all the ligands. These doublets/multiplets are due to aryl protons of benzene ring. However, a singlet at 11.695 *ppm* may be attributed to the phenolic -OH of the acyl pyrazolone ligand. The ^{1}H NMR spectral data are presented in

section 2. The ^{1}H NMR spectrum of ligand PMPAC is shown in Fig. S6. The ^{1}H NMR spectrum of Zn(II) complexes of **1** and **2** were recorded in deuterated DMSO, and ^{1}H NMR spectrum of Zn(II) complexes of **3** was recorded in $CDCl_3$ at room temperature shows signals consistent with the proposed structure. The multiplets around 7.0–7.9 *ppm* are assigned to aromatic protons, and propionyl protons of $–CH_2$- group at 2.556-2.611(q) *ppm*. The peak for phenolic –OH of the acylpyrazolone ligand is absent in the zinc(II) complexes which confirms deprotonation on complexation. The ^{1}H NMR spectral data are presented in section 2. The ^{1}H NMR spectrum of complex **3** is shown in Fig. S10.

In the ^{13}C NMR spectra of the ligands, the carbon atoms of the methyl groups appear in the range 15.72–21.02 *ppm*. The carbon atoms of the one benzene rings exhibit signals in the range 118.13–147.76 *ppm*. Eleven signals were observed for ligand PMPAC. Some of the signals might be overlapped as indicated by the intensity of a few signals. The other ligand MCPMPAC, where one of the benzene rings is *m*-substituted, show thirteen signals, as expected because of the loss of symmetry. All the protons and carbons were found as to be in their expected region. The ^{13}C NMR spectral data are shown in section 2. The ^{13}C NMR spectrum of ligand PMPAC is shown in Fig. S11.

The mass spectra of both bidentate pyrazolone ligands are in good agreement with proposed structures. The mass spectra of synthesized ligands were recorded and the obtained molecular ion peaks confirmed the proposed formula. Melting point of each ligand is high, as a result of this; the mass spectra were carried out by EI. The electronic impact mass spectra of PMPAC shows a molecular ion peak at m/z = 229.84 $[C_{13}H_{14}N_2O_2]^+$ with a relative intensity near to 100%, which is equivalent to its molecular weight. The electronic impact mass spectra of MCPMPAC shows a molecular ion peak at m/z = 264.34 $[C_{13}H_{13}ClN_2O_2]^+$ with a relative intensity near to 40.98%. The other peaks appeared in the mass spectra (abundance range 1–100%) are attributed to the fragmentation of ligand molecules obtained from the rupture of

different bonds inside the molecule. The mass spectral assignments for both the ligands are shown in the section 2. The mass spectral data of ligand PMPAC is shown in Fig. S13.

3.2. Crystal structure description

3.2.1. Complex 1

The molecular structure and the atom labeling scheme of the complex **1** is shown in Fig. 1. The main bond distances and angles are listed in Table 2.

As shown in Fig. 1, the Zn(II) ion is pentacoordinated by four oxygen atoms of two acyl pyrazolone ligands and one oxygen atom of water molecule. The two oxygen donors of both pyrazolone molecules occupy the basal sites of the pyramidal structure, whereas the water molecule binds the zinc at the apical site. In this complex, the incorporation of the solvent into the coordination sphere increases the coordination number to five and the geometry around the metal is now distorted trigonal bipyramidal.

In the complex, the zinc atom occupies a distorted trigonal bipyramidal environment (TBP), formed by four oxygen atoms [O(1), O(2), O(1_i), O(2_i)] supplied by two pyrazolone ligands (Symmetry code: (i) -x, y, 0.5-z). The fifth coordination site is occupied by one oxygen atom of water molecule. The Zn–O distances of the basal plan are Zn(1)-O(1)= 1.9934(16) Å and Zn(1)-O(2)= 2.0158(17) Å, whereas the axial distance of Zn(1)-O(3) is 2.011(3)Å. The longest distance does not correspond to the terminal Zn(1)-O(3), but instead to one of the basal Zn(1)-O(2) distance of the pyrazolone molecule.

All atoms of the chelate and pyrazolone rings lie almost in the same plane. One water molecule connects with the neighbouring pyrazolone-ring N(1) through intermolecular hydrogen bonds [O(3)–H(3)……N(1_i)]. H-bonding interactions play an important role in forming the supramolecular structure by self-assembly and stabilizing. The Hydrogen bonding geometry parameters of the complex are shown in Table 3.

In this complex the chlorine molecules are disordered at two positions. At C(8), occupancy of H(8) is 0.06 and Cl(1A) 0.94 (total 1). Similarly at C(10) occupancy of H(10) is 0.94 and Cl(1B), 0.06 (total 1). We have taken whole molecule except chlorine as part 1 and chlorine as part 2.

3.2.2. Complex 2

The structure of the complex **2** is illustrated in Fig. 1. Selected bond lengths and bond angles are listed in Table 2. Complex 2 is five-coordinate Zn(II) with one water molecule and four oxygens of two bidentate acylpyrazolonates. The coordination geometry may be described as slightly distorted trigonal bipyramidal. Zn exists in the location of the centre of symmetry. Four oxygens [O(16), O(16_i), O(17) and O(17_i)] from two PMPAC-composed equatorial planes, while one water molecule is axial. The angle of O(17)–Zn(1)–O(17_i) is 174.91(9)°. The angles of the O(17)–Zn(1)–O(16), O(17_i)–Zn(1)–O(16), O(16_i)–Zn(1)–O(16), O(17)–Zn(1)–O(1) and O(16)–Zn(1)–O(1) are 89.83(6)º, 88.43(6)º, 139.98(10)º, 92.55(4)º and 110.01(5)º, respectively (Symmetry code: (i) -x, y, 0.5-z). Moreover, the C(3)–N(2) bond length is close to the C–N double bond length, confirming that the keto form of the ligand tautomerizes to the enol form.

Zn(II) and the coordinated oxygens constitute two six-chelate rings which have the boat configuration. All atoms of the chelate and pyrazolone rings lie almost in the same plane. One water molecule connects with the neighbouring pyrazolone-ring N(2) through intermolecular hydrogen bonds O(1)–H(1)……N(2_i). H-bonding interactions play an important role in forming the supramolecular structure by self-assembly and stabilizing. The Hydrogen bonding geometry parameters of the complex are also shown in Table 3.

3.2.3. Complex 3

The molecular structure of complex **3** together with the atom-numbering scheme is illustrated in Fig. 1. Important bond lengths and angles are listed in Table 2. The X-ray analysis revealed that the complex was a 6-coordinate mononuclear Zn(II) complex with two nitrogen atoms of the phenanthroline molecule and four oxygen atoms of two bidentate pyrazolonates. Taking into consideration that it usually adopts an octahedral conformation because of the large ligand field stabilization energy, this configuration is quite ideal. The coordination plane around Zn(1) ion is composed of O(1), O(2) and N(16) atoms with normal bond distances of Zn(1)–O(1): 2.1123(14)Å, Zn(1)–O(2): 2.0347(13)Å and Zn(1)–N(16): 2.1908(16)Å. In the equatorial plane, the trans angles in O(1)–Zn(1)–O(1_i) and O(2)–Zn(1)–N(16) are around 180º, while 90.35(6)º for O(2)–Zn(1)–O(1_i), 91.45(6)º for O(2_i)–Zn(1)–N(16), 97.70(6)º for O(1)–Zn(1)–N(16_i) and 84.86(6)º for the angle O(1)–Zn(1)–N(16), add up to 364.36(6)º. Bond angles show that the coordination geometry around the zinc ion in the complex is distorted octahedral. Atoms O(1), O(2), O(1_i) and N(16) of the ligand molecules occupy the equatorial positions around the metal centre. Atoms N(16_i) and O(2_i) of the ligands occupy axial positions creating a octahedral geometry around the central metal.

In the complex, the bond length of O(2)–C(3) and O(1)–C(13) are 1.272(2) and 1.245(3) Å, respectively, which are shorter than 1.43 Å for a C–O single bond and longer than 1.22 Å for a C=O double bond length. Moreover, the C(3)–N(2) bond length is close to the C–N double bond length, confirming that the keto form of the ligand tautomerizes to the enol form. All atoms of the complex and the pyrazolone rings are not in the same plane. As a result, the complex is a non-planar molecule. As this complex has no solvent molecule, H-bonding is absent in this complex. In Complex 3 also, methyl group is disordered over two sets of sites in a 0.75(2):0.25(2) ratio.

3.3. DNA binding studies

Many workers [26, 27] were of the opinion that the two major binding modes of interaction of substrate with DNA were (a) the intercalation: wherein the metal complexes squeeze in between the double helix through hydrogen bonding and (b) the covalent binding: where two major sites are available for the metal ion to interact with the DNA, one being the electron donor groups of the bases, more preferably at the guanine N-7 and the other the phosphate moieties of the ribose phosphate backbone.

3.3.1. Electronic absorption titration

The application of electronic absorption spectroscopy in DNA binding studies is one of the most useful techniques carried out at 25 ± 2ºC. The binding of the metal complexes to DNA helix is often characterized through absorption spectral titration, followed by the changes in the absorbance and shift in the wavelength. The electronic spectra of Zn(II) complexes titrated with DNA are given in Fig. 2. Hyperchromism and hypochromism are the spectral changes typical of a metal complexes association with the DNA helix [20]. Absorption titration experiments were performed by maintaining the metal complex concentration as constant at 5 μM while varying the concentration of the DNA within 0–75 μM. Upon the addition of DNA, interesting changes in the absorbencies of the *d–d* transition absorption bands of the complexes were observed. The observed hyperchromism for all the complexes unambiguously revealed the active participation of pyrazolone moieties in association with the DNA. However, the lack of red shift suggests that the binding mode of both the complexes was not classical intercalation. Because of the bulky structure of the complexes, the aromatic rings cannot completely intercalate. Therefore, the observed spectral changes were rationalized in terms of partial intercalation.

To further illustrate the DNA binding strength, the intrinsic binding constant K_b was determined from the non-linear DNA/E_a-E_f *vs* [DNA] for all three complexes (**1**, **2** & **3**) and

they were found to be 1.24×10^5 M^{-1}, 0.52×10^5 M^{-1} and 0.88×10^5 M^{-1}, respectively. Binding constants of these complexes were lower in comparison to those observed for typical classical intercalators (ethidium–DNA, $1.4 \times 10^6 M^{-1}$) [21]. The diminution of the intrinsic binding constant s could be explained by the steric constraints imposed by the ligand framework and thus encouraging a partial intercalation binding mode for the complexes. Our results are consistent with earlier reports on preferential binding to DNA in the Zn complexes [28].

Fluorescence spectral technique using the emission intensity of ethidium bromide (EB) bound to DNA has been used to determine the binding propensity of the complexes. No luminescence was observed for the complex solution, either with or without the presence of DNA. So, the binding of complex and DNA cannot be directly presented in the emission spectra. Ethidium bromide (EB) is a weak fluorophore, but its emission intensity in the presence of DNA can be greatly enhanced because of its strong intercalation between the adjacent DNA base pairs. EB, a planar aromatic heterocyclic dye intercalates non specifically into the DNA which causes it to fluoresce strongly.

If the complexes can intercalate into DNA, the binding sites of DNA available for EB will be decreased, and hence the fluorescence intensity of EB will be quenched [29]. In our experiments, as depicted in Fig. 3 for complexes **1**, **2** and **3**, the fluorescence intensity of EB show a remarkable decreasing trend with the increasing concentration of the complexes, indicating that some EB molecules are released from EB-DNA complex after an exchange with the complexes, which result in the fluorescence quenching of EB. This may be due eiter to the metal complex competing with EB for the DNA-binding sites thus displacing the EB (whose fluorescence is enhanced upon DNA binding) or it should be a more direct quenching interaction on the DNA itself. We assume the reduction of the emission intensity of EB on increasing the complex concentration could be caused due to the displacement of the DNA

bound EB by the Zn(II) complexes. Such a quenched fluorescence behavior of EB bound to DNA caused by the interaction between Zn(II) complexes and DNA is also found in other zinc complexes [30].

The fluorescence quenching curve of EB bound to DNA by the Zn (II) complexes are shown in Fig. 4. The ratio of the slope to the intercept obtained by plotting F_0/F versus [Complex] yielded the value of K_{sv} corresponding to the three complexes as 3.21×10^3 M^{-1}, 0.86×10^3 M^{-1} and 0.91×10^3 M^{-1}, respectively. Values of K_{sv} suggested that the complex **1** showed higher quenching efficiency than the other complexes **2** and **3**. Further, the figures also show that the ratio of quenching of the intensities in all three complexes is different, reflecting more binding of complex **1** with DNA to leach out more number of EB molecules originally bound to DNA than that of the complexes **2** and **3**. Our results are consistent with earlier reports on preferential binding to DNA in the Zn(II) complexes [31–32]. All these results showed clearly that the complex **1** possesses strong tendency to bind with DNA which is consistent with the viscosity results.

In addition to spectroscopic titrations, viscosity measurements were carried out to provide further information on the nature of the interaction between the complex and DNA. A classical intercalation model demands that the DNA helix lengthens as base pairs are separated to accommodate the bound ligand leading to an increase of the DNA viscosity. In contrast, semi-intercalation of a ligand could bend or kink the DNA helix, and thus reduce its effective length and, concomitantly, its viscosity. A classical intercalation mode causes a significant increase in viscosity of DNA due to an increase in separation of base pairs at intercalation sites and hence an increase in overall DNA length [33].

The changes in the relative viscosity of rod-like DNA in the presence of Zn(II) complexes are shown in Fig. 5. The viscosity of DNA increases greatly with increasing concentration of complex, which is similar to that of the proven intercalator EB [34]. This

observation suggests that the principal mode of DNA binding by complexes involve base-pair intercalation, with one ligand intercalating into the base pairs and the other ligand being left outside the helix [35]. The results obtained in this study are consistence with similar studies done by others [36-38]. The intercalative interaction with DNA is related to the molecular structure, as in these complexes there is a little distorted plane that may lead to the weak intercalative mode. This result also parallels the pronounced emission enhancement of the complexes, and is comparable with the proven classical intercalator EB. On the basis of the viscosity results, the complexes bind with DNA through the intercalation mode [7].

Conclusion

The 4-acyl pyrazolone ligands have been prepared by the acylation of pyrazolone derivatives with propionyl chloride. They have been characterized by IR, ^{1}H NMR, ^{13}C NMR and mass spectrometry. Binary and mixed-ligand Zn(II) complexes of these ligands have been synthesized and characterized by metal estimation, molar conductance, IR, ^{1}H NMR and single crystal X-ray study. The data shows that they have composition of the type [$ZnL_2.H_2O$] and [ZnL_2(Phen)]. The X-ray analyses and NMR spectra of the complexes show that the Zn(II) ion center in [ZnL_2(Phen)] is six-coordinated while the Zn(II) ion center in [$ZnL_2.H_2O$] is five-coordinated. The lower molar conductance values of the complexes reveals that these complexes are non electrolytes. The DNA-binding properties of the synthesized complexes have been examined by absorption spectroscopy, fluorescence spectroscopy and viscosity measurements. Evidences have suggested that the complexes could interact with DNA *via* partial intercalative mode. Furthermore, in the EB competition absorption titration assay, the binding constants for the complexes, K_{sv} are obtained, which are 3.21×10^{3} M^{-1} for **1**, 0.86×10^{3} M^{-1} for **2** and 0.91×10^{3} M^{-1} for **3,** respectively. The results indicate that complex **1** has a greater DNA affinity than **2** and **3**. Moreover, complex **1** can strongly bind to DNA through intercalation, while **2** and **3** binds to DNA in a partial intercalative mode.

Acknowledgement

The authors are thankful to University Grants Commission, New Delhi for the financial assistance to this work in terms of major research project [Project F.37-376/2009 12.01.2010(SR)] to RNJ. They are also thankful Head, Department to of Chemistry for providing necessary facilities required carrying out this work.

Supporting information

CIF files for the X-ray crystal structures have been deposited with the Cambridge Crystallographic Data Center (CCDC, 931119**-1**, 910379**-2**, 929473**-3**). Copies of this information can be obtained free of charge at www.ccdc.cam.ac.uk/conts/retrievel.html or from the CCDC, 12 Union Road, Cambridge CB2 1EZ, UK; fax : +44-1223/336-033. email: deposit@ccdc.ac.uk.

References

[1] (a) M.A.S. Goher, M.R. Saber, R.G. Mohamed, A.K. Hafez, F.A. Mautner, J. Coord. Chem. 62 (2009) 234-241; (b) M.A.S. Goher, F.A. Mautner, B. Sodin, B. Bitschnau, J. Mol. Struct. 879 (2008) 96-101.

[2] (a) M. Eddaoudi, D.B. Moler, H. Li, B. Chen, T.M. Reineke, M. O'Keeffe, O.M. Yaghi, Acc. Chem. Res. 34 (2001) 319-330; (b) S.L. James, Chem. Soc. Rev. 32 (2003) 276-288.

[3] (a) D. Kovala-Demertzi, S.K.A. Hadjikakou, M. Demertzis, Y. Deligiannakis, J. Inorg. Biochem. 69 (1998) 223-226; (b) N. Sridevi, K.K.M. Yusuff, Toxi. Mech. Meth. 17 (2007) 559-565; (c) N.P.A. Seedher, Drug Metabol. Drug Interact. 25 (2010) 17-24.

[4] MIMS India, vol. 17, 1997, p 217.

[5] (a) R.A. Bailey, T.R. Peterson, Can. J. Chem. 47 (1969) 1681-1687; (b) V. Mahalingam, N. Chitrapriya, F.R. Fronczek, K. Natarajan, Polyhedron 29 (2010) 3363-3371; (c) S.N. Shukla, P. Gaur, H. Kaur, M. Prasad, R.S. Srivastava, J. Coord. Chem. 61 (2008) 1875-1883 ;

(d) Q. Wang, M.-J. Wu, E.-C. Yang, X. -G Wang, X.-J. Zhao, J. Coord. Chem. 61 (2008) 595-604; (e) P. Mayer, E. Hosten, K. Potgieter, T. Gerber, J. Chem. Crystallogr. 40 (2010) 1146-1149.

[6] S. Parihar, Soyeb Pathan, R. N. Jadeja, A. Patel, V. K. Gupta, Inorg. Chem., 51 (2012) 1152-1161.

[7] R.N. Jadeja, K.M. Vyas, V.K. Gupta, R.G. Joshi, C. Ratna Prabha, Polyhedron 31 (2012) 767–778.

[8] K.M. Vyas, R.G. Joshi, R.N. Jadeja, C.R. Prabha, V.K. Gupta, Spectrochim. Acta A 84 (2011) 256–268.

[9] K.M. Vyas, R.N. Jadeja, V.K. Gupta, K.R. Surati, J. Mol. Struct. 990 (2011) 110–120.

[10] B. T. Thaker, Kiran R. Surati, Shantilal Oswal, R. N. Jadeja, Vivek K. Gupta, Struct Chem 18 (2007) 295–310.

[11] R. N. Jadeja, N. J. Parmar, Synthesis and Reactivity in Inorganic, Metal-Organic and Nano-Metal Chemistry. 35 (2005) 111–117.

[12] R.N. Jadeja, J.R. Shah, E. Suresh, P. Paul, Polyhedron 23 (2004) 2465–2474.

[13] W. L. F. Armarego, D.D. Perrin, Purification of Laboratory Chemicals, fourth ed., The Bath Press, Butterworth–Heinemann Publication, 1997.

[14] Bruker, SMART (Version 5.631), SAINT (Version 6.45) and SADABS (Version 2.05). Bruker AXS Inc., Madison, Wisconsin, USA, 2003.

[15] G. M. Sheldrick, SHELXS97 and SHELXL97, Germany, University of Gottingen, 1997.

[16] C. K. Johnson, ORTEP II; Report ORNL-5138, Oak Ridge National Laboratory, Oak Ridge, TN, 1976.

[17] A. L. Spek, PLATON for Windows. September 1999 Version, University of Utrecht, Netherlands, 1999.

[18] M. Nardelli, J. Appl. Cryst., 28 (1995) 659.

[19] M. E. Reichmann, S. A. Rice, C. A. Thomas, P. Doty, J. Am. Chem. Soc., 76 (1954) 3047-3053.

[20] S. S. Bhat, A. A. Kumbhar, H. Heptullah, A. A. Khan, V. V. Gobre, S. P. Gejji, V. G. Puranik, Inorg. Chem. 50 (2011) 545–558.

[21] J. R. Lakowicz, Principles of Fluorescence Spectroscopy; 3rd ed. Springer Science+Business Media: New York, 2006.

[22] J.B. Chaires, N. Dattagupta, D.M. Crothers, Biochemistry 21 (1982) 3933–3940.

[23] W.J. Geary, Coord. Chem. Rev. 7 (1971) 81–122.

[24] E.C. Okafo. Spectrochim. Acta, Part A, 37 (1981) 945-950.

[25] Xin Hu, Li Zhang, Lang Liu, Guangfei Liu, Dianzeng Jia, Guancheng Xu, Inorg.Chim.Acta 359 (2006) 633-341.

[26] P. Uma Maheswari, M. Palaniandavar, Inorg. Chim. Acta 357 (2004) 901–912.

[27] D. Wettig, D.O. Wood, J.S. Lee, J. Inorg. Biochem. 94 (2003) 94–99.

[28] Yuan Wang, Zheng-Yin Yang, Transition Metal Chemistry 30 (2005) 902–906.

[29] R. Indumathy, S. Radhika, M. Kanthimathi, T. Weyhermuller, B.U. Nair, J. Inorg. Biochem. 101 (2007) 434-443

[30] N. Ramana, A. Selvana, P. Manisankar, Spectrochimica Acta A 76 (2010) 161-173.

[31] F. Arjmand, M. Aziz, Eur. J. Med. Chem. 44 (2009) 834-844.

[32] N. Raman, R. Jeyamurugan, S. Sudharsan, L. Mitu, Arabian journal of chemistry 6 (2010) 235-247.

[33] X.H. Zou, B.H. Ye, H. Li, Q.L. Zhang, H. Chao, J.G. Liu, L.N. Ji, X.Y. Li, J. Biol. Inorg. Chem. 6 (2001) 143-150.

[34] Q.-L. Zhang, J.-G. Liu, H. Chao, G.-Q. Xue, L.-N. Ji, J. Inorg. Biochem. 83 (2001) 49-55.

[35] P. Xi, Z. Xu, F. Chen, Z. Zeng, X. Zhang, J. Inorg. Biochem. 103 (2009) 210-218.

[36] N. Raman, R. Jeyamurugan, M. Subbulakshmi. Chem. Papers 64 (2010) 318–328.

[37] Z. Y. Yang, B. D. Wang. J. Organomet. Chem. 691 (2006) 4159-4166.

[38] R.N. Jadeja, Sanjay Parihar, Komal Vyas. J. Mol. Struct. 1013 (2012) 86-94.

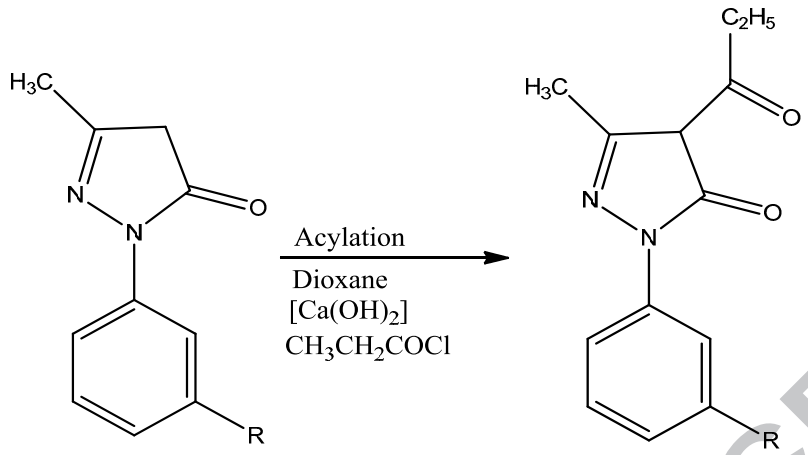

Where R = H, Cl

Scheme 1. Synthesis of acyl Pyrazolone ligands

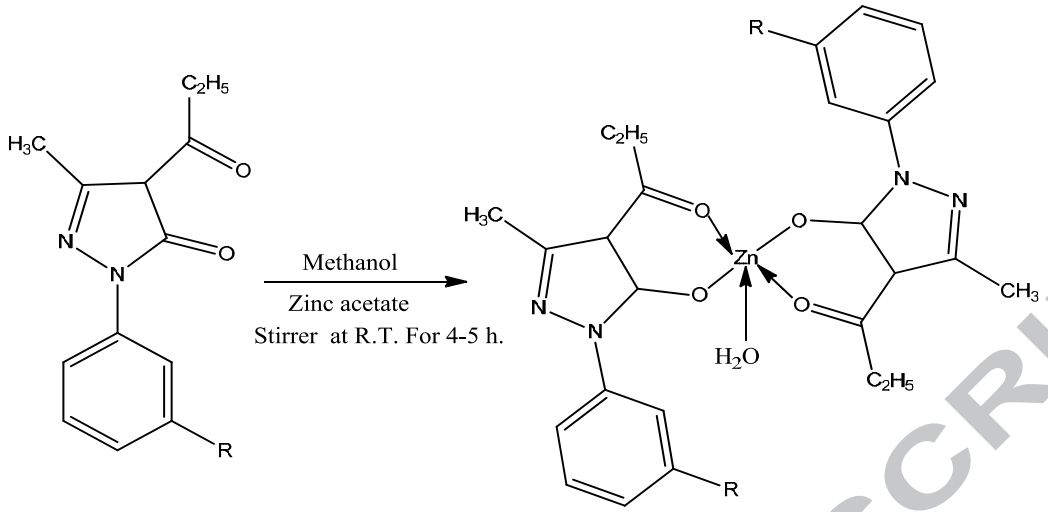

Where, (**1**):R = Cl (**2**):R = H

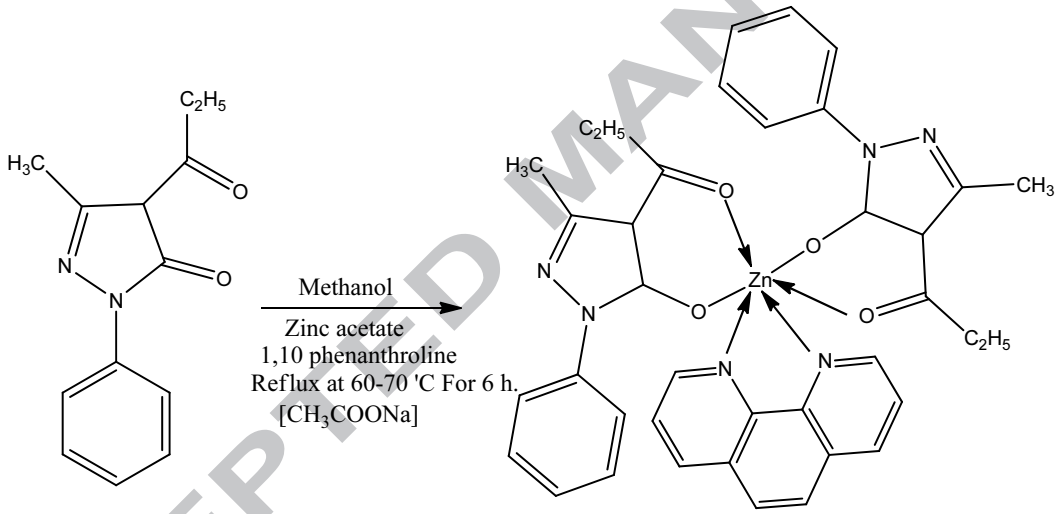

Scheme 2. Synthesis of complexes

539

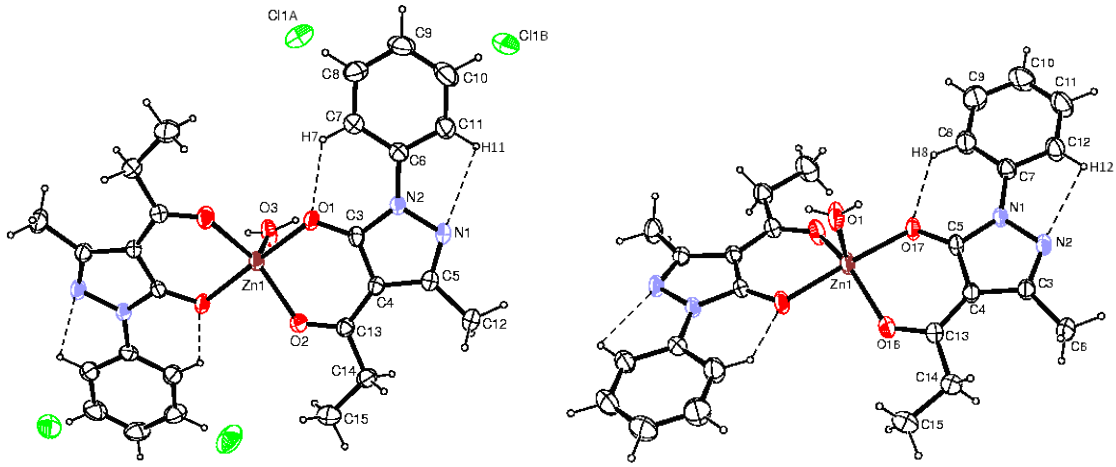

540 **(A)** **(B)**

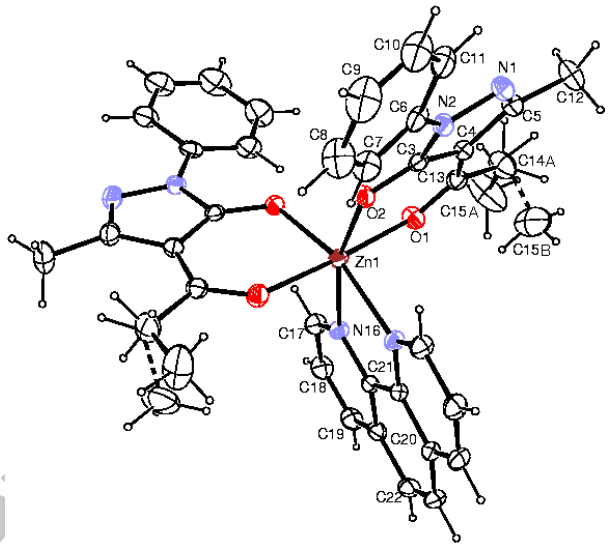

541

542 **(C)**

543

544 Fig. 1. ORTEP view of the Complex **1(A),** Complex **2(B)** and Complex **3(C)** showing atom-
545 labelling scheme. Displacement ellipsoids are drawn at the 50% probability level and H
546 atoms are shown as small spheres of arbitrary radii.

547

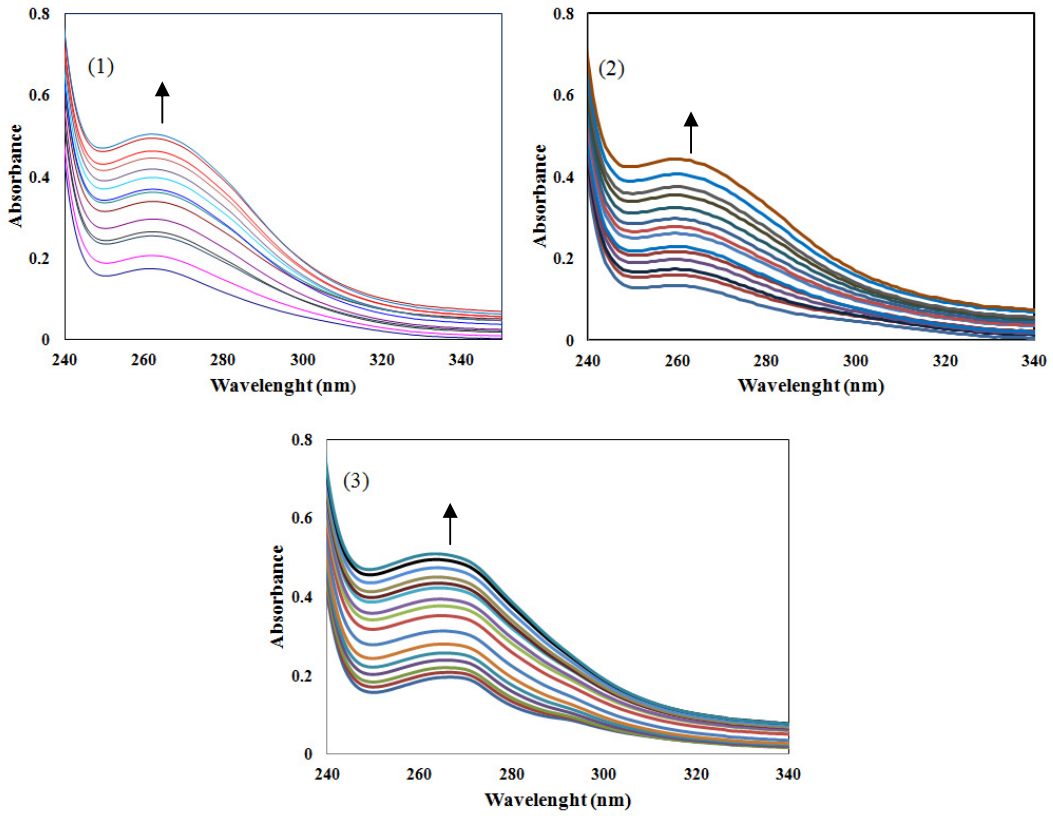

Fig. 2. Electronic spectra of complexes (1) Complex **1**, (2) Complex **2** and (3) Complex **3** in DMF in the absence and presence of CT-DNA. Arrow shows the absorbance changes upon increasing DNA concentrations.

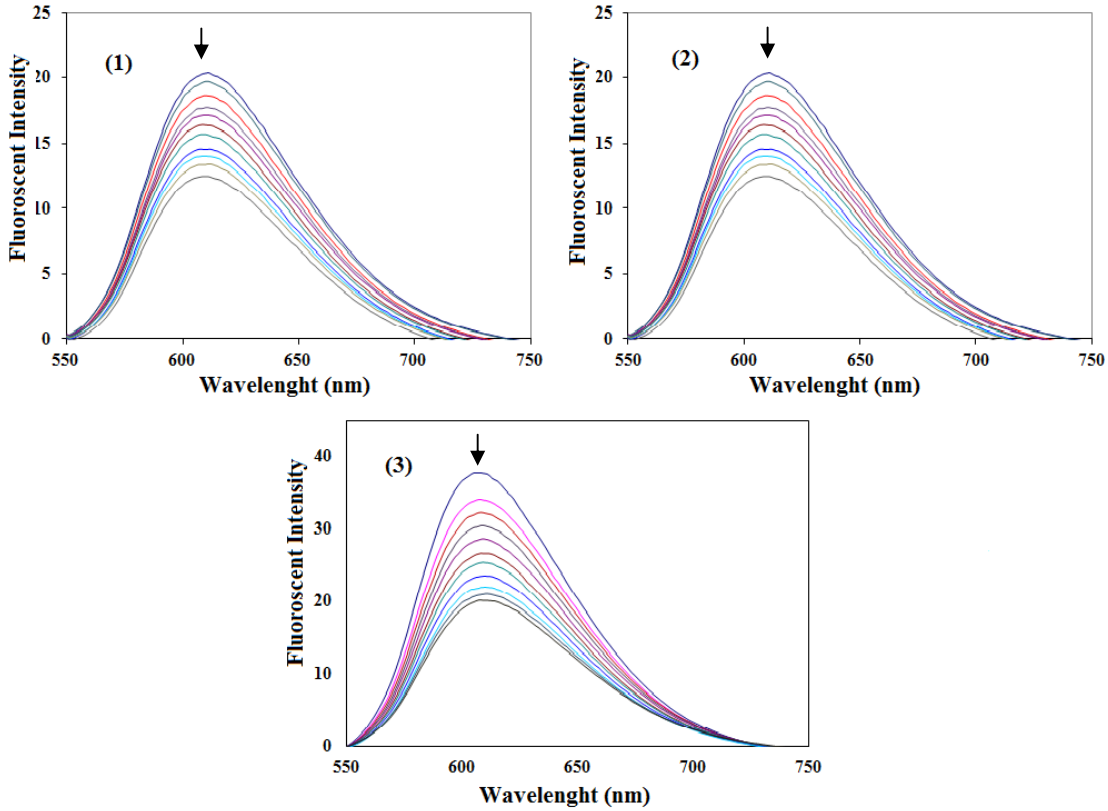

Fig. 3. Emission spectra of EB bound to DNA in the absence and presence of complexes (1) Complex **1,** (2) Complex **2** and (3) Complex **3**. The arrow shows the intensity changes on increasing the complex concentration.

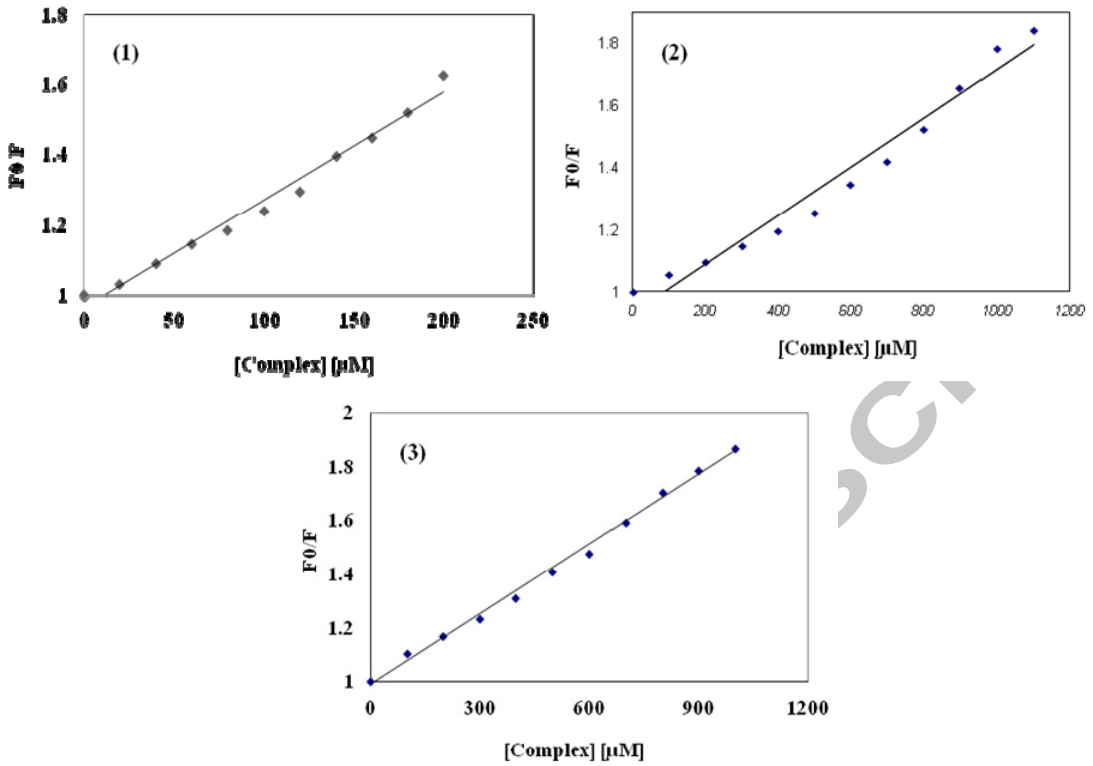

Fig. 4. Fluorescence quenching curve of EB bound to DNA by (1) Complex **1,** (2) Complex **2** and (3) Complex **3**.

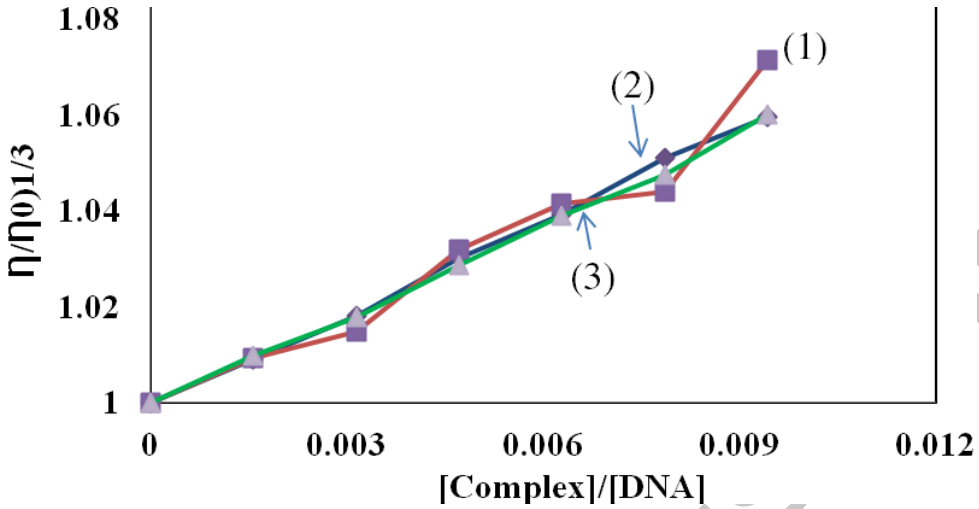

Fig. 5. Effect of increasing amounts of (1) Complex **1,** (2) Complex **2** and (3) Complex **3** on the relative viscosities of CT-DNA at 30.0 ± 0.1 ºC. [DNA] = 3 mM, [Complex]/[DNA] = 0, 0.0015, 0.0031, 0.0047, 0.0062, 0.0078, 0.0094 respectively.

Table 1: Summary of crystallographic data

Compound	Complex **1**	Complex **2**	Complex **3**
Chemical formula	$C_{26}H_{26}Cl_2N_4O_5Zn$	$C_{26}H_{28}N_4O_5Zn$	$C_{38}H_{34}N_6O_4Zn$
Formula weight (g mol^{-1})	610.78	541.89	704.08
Crystal system	Monoclinic	Monoclinic	Monoclinic
Crystal size	0.3× 0.2× 0.2	0.3× 0.2× 0.2	0.3× 0.2× 0.2
density (calcd) (g cm^{-3})	1.529	1.445	1.353
Crystal description	White Block	White Block	Colourless Block
a (Å)	26.8009(11)	26.2269(12)	22.1967(7)
b (Å)	7.2535(3)	7.2955(2)	10.0616(3)
c (Å)	15.0462(6)	15.0463(6)	16.7807(6)
α (°)	90.00	90.00	90.00
β (°)	114.892(5)	120.113(6)	112.697(4)
γ (°)	90.00	90.00	90.00
Z	4	4	4
V (Å^3)	2653.26(19)	2490.4(2)	3457.48(19)
Wavelength	0.71073 Å	0.71073 Å	0.71073 Å
Reflection collected	15998	28625	25112
Observed reflections	2024	2053	2988
R_{int}	0.0521	0.0556	0.0407
R_σ	0.0366	0.0247	0.0227
Number of parameters	190	170	233
Space group	C 2/c	C 2/c	C 2/c
Absorption coefficient μ (cm^{-1})	1.172	1.031	0.760
F (000)	1256	1128	1464
Temperature (°C)	293(2)	293(2)	293(2)
Goodness-of-fit (GOF) on F^2	1.031	1.031	1.066
R1/wR2([I > 2r (I)]	0.0376/0.0838	0.0313/ 0.0776	0.0350/0.0837
R1/wR2 (all data)	0.0544/0.0904	0.0410/ 0.0822	0.042/0.0884

Table 2: Important bond lengths and angles for the complexes.

Bond distances (Å) with esd's in parentheses		Bond angles (°) with esd's in parentheses	
Complex **1**			
Zn1 – O1	1.9934(16)	O1 – Zn1 – O(1_i)	173.68(12)
Zn1 – O3	2.011(3)	O1 – Zn1 – O3	93.16(6)
Zn1 – O2	2.0158(17)	O1 – Zn1 – O2	89.70(7)
O1 – C3	1.264(3)	O1 – Zn1 – O(2_i)	88.25(7)
O2 – C13	1.257(3)	O3 – Zn1 – O2	108.91(6)
N1 – C5	1.310(3)	O2 – Zn1 – O(2_i)	142.19(12)
N1 – N2	1.396(3)	C3 – O1 – Zn1	121.82(16)
N2 – C3	1.374(3)	C13 – O2 – Zn1	129.74(17)
N2 – C6	1.412(3)	C5 – N1 – N2	106.35(18)
O3 – H3	0.85(3)	O2 – C13 – C14	116.6(2)
C3 – C4	1.417(3)	N2 – C3 – C4	106.14(19)
C4 – C5	1.425(3)	Zn1 – O3 – H3	123(2)
C4 – C13	1.425(3)	O1 – C3 – C4	130.9(2)
C13 – C14	1.495(3)	O1 – C3 – N2	122.9(2)
Complex **2**			
Zn1 – O17	2.0050(13)	O17 – Zn1 – O(17_i)	174.91(9)
Zn1 – O16	2.0071(14)	O(17_i) – Zn1 – O16	88.43(6)
Zn1 – O1	2.008(3)	O17 – Zn1 – O16	89.83(6)
O16 – C13	1.253(2)	O(16_i) – Zn1 – O16	139.98(10)
O17 – C5	1.270(2)	O17 – Zn1 – O1	92.55(4)
N1 – C5	1.372(2)	O16 – Zn1 – O1	110.01(5)
N1 – N2	1.399(2)	C13 – O16 – Zn1	129.56(13)
N1 – C7	1.418(2)	C5 – O17 – Zn1	121.39(13)
N2 – C3	1.305(3)	C5 – N1 – N2	110.75(15)
C3 – C4	1.430(2)	O17 – C5 – N1	122.96(18)
C3 – C6	1.493(3)	N2 – C3 – C4	111.62(17)
C4 – C5	1.413(3)	O16 – C13 – C4	121.95(18)
C4 – C13	1.421(3)	N1 – C5 – C4	106.25(15)
C13 – C14	1.500(3)	C12 – C7 – N1	119.71(18)
Complex **3**			
Zn1 – O2	2.0347(13)	O(2_i) – Zn1 – O2	102.56(8)
Zn1 – O1	2.1123(14)	O2 – Zn1 – O(1_i)	90.35(6)
Zn1 – N16	2.1908(16)	O2 – Zn1 – O1	87.64(5)
O1 – C13	1.245(3)	O(1_i) – Zn1 – O1	176.79(8)
O2 – C3	1.272(2)	O2 – Zn1 – N16	164.15(6)
N1 – C5	1.304(3)	(O2_i) – Zn1 – N16	91.45(6)
N1 – N2	1.395(3)	O1 – Zn1 – N(16_i)	97.70(6)
N2 – C3	1.376(2)	O1 – Zn1 – N16	84.86(6)
N2 – C6	1.411(3)	N16 – Zn1 – N(16_i)	75.78(8)
N16 – C17	1.324(2)	C13 – O1 – Zn1	130.89(14)
N16 – C21	1.354(2)	C3 – O2 – Zn1	123.22(12)
C4 – C13	1.422(3)	C5 – N1 – N2	105.63(17)
C17 – C18	1.393(3)	C17 – N16 – Zn1	127.42(14)
		C21 – N16 – Zn1	114.49(12)

597
598
599
600 **Table 3: Hydrogen–bonding geometry (esd's in parentheses)**

Complex	**D–H…A**	**d(D-H)/Å**	**d(H-A)/Å**	**d(D-A)/Å**	**D-H-A/°**
Complex-1	C7-H7-O(1_i)	0.93	2.17	2.808(4)	125
	C11-H11-N(1_i)	0.93	2.47	2.806(4)	101
	O3-H3-N(1_i)	0.85(4)	1.94(3)	2.781(3)	170(3)
Complex-2	C8-H8...O(17_i)	0.93	2.20	2.840(3)	125
	C12-H12...N(2_i)	0.93	2.45	2.798(3)	102
	O1-H1...N(2_i)	0.74(3)	2.04(3)	2.772(2)	174(2)

601 Symmetry code : (i) ^{1}+X,+Y,+Z (ii) ^{2}-X,2-Y,-Z for Complex-1 (i) ^{1}+X,+Y,+Z (ii) ^{2}+X,-Y,1/2+Z for Complex-2

602

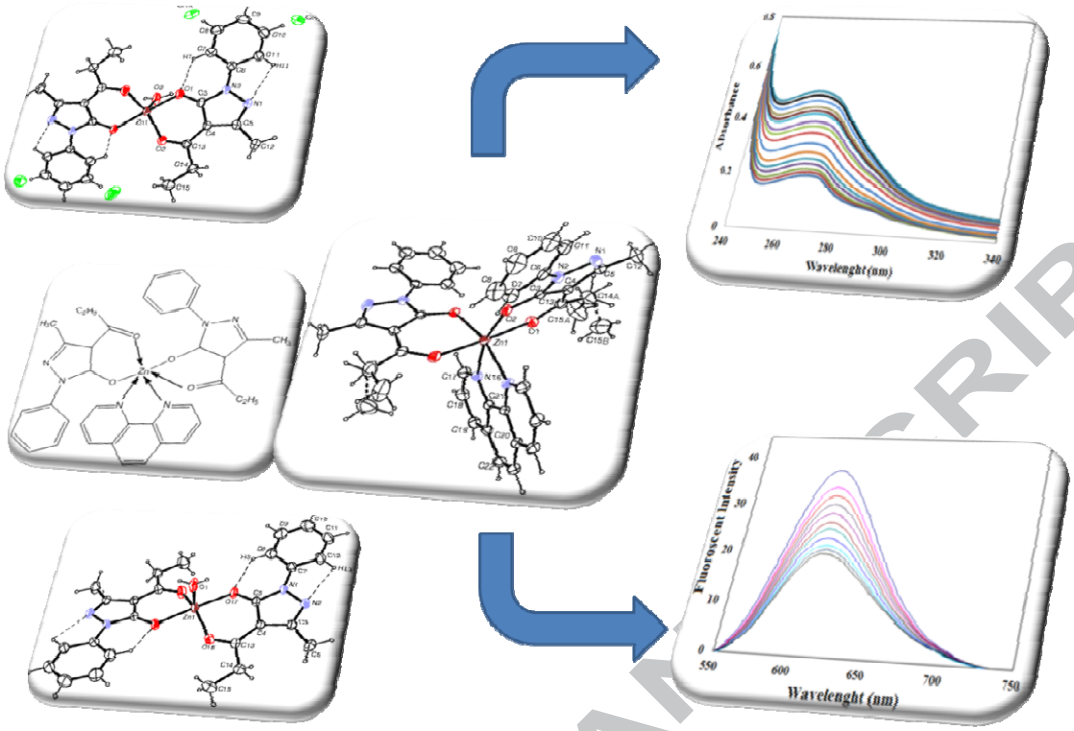

603

A series of three new Zn(II) coordination complexes has been synthesized using propionyl pyrazolone ligands, 1, 10, phenanthroline and zinc acetate. The structural features of synthesized complexes were determined by different techniques including single crystal X-ray studies. DNA-binding studies of the synthesized complexes with CT-DNA have been carried out by spectroscopic methods and viscosity measurements. Experimental results suggest that the zinc complexes have the ability to form adducts with DNA and to distort the double helix by changing the base stacking.